Research Article

IT Medical Team
http://www.imedpub.com

Health Science Journal
ISSN 1791-809X

2024
Vol. 18 No. S10: 002

Design and Performance Analysis of a Novel Hollow Core-Based Photonic Crystal Fiber for Edible Oil Sensing in the Terahertz (THz) Regime

Jannatun Ferdous*, Md. Dulal Haque, Md. Selim Hossain, Md.Abubakar Siddik, Md. Mahfujur Rahman

Department of Electronics and Communication Engineering, Hajee Mohammad Danesh Science and Technology University, Dinajpur, Bangladesh

Corresponding author:
Jannatun Ferdous, Department of Electronics and Communication Engineering, Hajee Mohammad Danesh Science and Technology University, Dinajpur, Bangladesh

E-mail: jannatun.tee@gmail.com

Citation: Ferdous J, Haque MD, Hossain SM, Siddik AM, Rahman MM (2024) Design and Performance Analysis of a Novel Hollow Core-Based Photonic Crystal Fiber for Edible Oil Sensing in the Terahertz (THz) Regime. Health Sci J Vol. 18 No.S10:002.

Abstract

This work proposes a Hexagonal-core Photonic Crystal Fiber (H-PCF) based edible oil sensor in the Terahertz (THz) range (1.0 THz ≤ f ≤ 3.0 THz) and different sensing characteristics are numerically analyzed. The suggested sensor's performance was assessed by means of COMSOL multi physics, a commercial program that uses the Full Vector Finite Element Method (FV-FEM). The computational results indicate that the relative sensitivity is 85.591%, 84.648%, 82.625%, 82.683%, and 79.161%, respectively, at f=2.2 THz, for several types of sunflower oil, mustard oil, coconut oil, olive oil and palm oil; and the corresponding effective areas are 7.22×10^{-8} m^2, 7.09×10^{-8} m^2, 6.83×10^{-8} m^2, 7.09×10^{-8} m^2, 6.5231×10^{-8} m^2. In addition, the effective material loss for sunflower oil, muster oil, coconut oil, olive oil, and palm oil has been found to be 0.02561 cm^{-1}, 0.027054 cm^{-1}, 0.030322 cm^{-1}, 0.028854 cm^{-1}, 0.035427cm^{-1} respectively. Moreover, the proposed sensor also has low confinement loss are 1.55×10^{-8} dB/m, 1.63×10^{-8} dB/m, 1.31×10^{-8} dB/m, 1.99×10^{-8} dB/m, 4.0345×10^{-8} dB/m. This proposed sensor can be fabricated using extrusion and 3D-printing technologies, and due to its augmented detecting capabilities, this proposed sensor can be used in edible oil sensing, food and beverage industry as well as various polarization maintaining terahertz application.

Keywords: Photonic crystal fiber; Edible oil sensor; Sensitivity; Confinement loss; Effective material loss

Received: 28-Mar-2024, Manuscript No. IPHSJ-24-14706; **Editor assigned:** 01-Apr-2024, PreQC No. IPHSJ-24-14706 (PQ); **Reviewed:** 15-Apr-2024, QC No IPHSJ-24-14706; **Revised:** 22-Apr-2024, Manuscript No. IPHSJ-24-14706 (R); **Published:** 29-Apr-2024, DOI: 10.36648/1791-809X.16.S10.002

Introduction

Edible oils are one of the vital sources of fat in our diet. It is not merely a cooking ingredient but a major component of human nutrition, culinary diversity, and cultural heritage. Its significa nce extends beyond the kitchen, influencing health outcomes, societal customs, and gustatory pleasures around the world. The highly consumable edible oils are olive, muster, soybean, canola, and sunflower oil. It offers several health advantages, particularly for the skin, bone, brain and heart. It also includes omega-3 fatty acids and polyunsaturated fatty acids, both of which are beneficial to heart health, cognitive function and immunity [1]. This frying oil also includes vitamin k, which is essential for blood contraction, bone metabolism management and bone mass maintenance [2]. On the other hand, as soybean oil also includes omega-6 fatty acids, it might have certain adverse consequences when used excessively in food preparation. Unfortunately, a few fraudulent companies offer contaminated oil, resulting in a number of adverse health risks. However, since the colors of the cooking oils are almost identical, it is difficult to distinguish between them. Low-cost cooking oils (palm oil) are sometimes disguised as high-cost oils (mustard oil, sunflower oil, etc.) by adding color or chemical compounds that are toxic to humans. As a result, detecting pure edible oil is critical for reducing health risks and maintaining a healthy lifestyle [1]. Existing oil sensing methods often suffer from limitations such as low sensitivity, poor selectivity, and lack of real-time monitoring capabilities. These limitations pose significant challenges for environmental monitoring, oil spill detection, and industrial processes, impacting both environmental sustainability and industrial safety. There is a critical need for advanced sensing solutions capable of addressing these challenges and providing reliable and efficient

oil detection and analysis capabilities. Photonic Crystal Fibers (PCFs) have gained much popularity in telecommunication and sensing applications because of their numerous remarkable optical properties, such as higher core power fraction, higher sensitivity, larger birefringence, lower effective material loss, lower scattering loss, etc. Since its development in 1996 [1], the proposed sensor aims to develop an innovative sensing system based on PCF technology for the detection and analysis of oil contaminants in various environments. Photonic Crystal Fiber (PCF) has provided novel possibilities for improving photonic instruments for sensing and communication applications. The design of this kind of glass fiber offers the implementation of a wider range of optical properties, including indefinite single-mode operation, a higher effective core area, increased transparency, design flexibility, and low loss [1-10].

On the contrary, owing to their high sensitivity and small size, PCF-based sensor devices were used in a variety of potential real-world applications, such as chemical sensing, biological tissue diagnosis, cancer cell detection, etc. [3]. Due to its multiple prospective applications, a small region in the electromagnetic spectrum (0.1 to 10 THz) has recently gained widespread attention and is termed the Terahertz (THz) radiation band [1]. Because this radiation band is between the infrared and microwave regions, it is often employed with no negative effects on humans or the environment [10]. As air lacks the absorbent qualities of this spectral range, it was first utilized as a medium for transmitting THz signals. Despite this, major issues such as dispersion, isolation, and transmitter-receiver alignment occurred when transmitting THz signals over long distances [11]. Several waveguides, such as parallel plate waveguides, metal waveguides, hollow-core waveguides, and PCFs, have been proposed to provide effective signal transmission throughout this spectral range [12-14]. THz PCF waveguide has higher transmission qualities than other waveguides because it absorbs less energy [15,16]. As a result, PCFs become a crucial component in THz signal's transmission and these waveguides were recommended as sensors for various applications [17-21].

Bikash Kumar Paul et al. presents a study on a Quasi-Photonic Crystal Fiber (Q-PCF) designed for Terahertz (THz) spectrum chemical sensing, focusing on high relative sensitivity. It details the design, theoretical background, and numerical analysis of the Q-PCF using full-vector finite element method-based simulations. The sensor demonstrates improved sensitivity for detecting analytes like ethanol, benzene, and water, with relative sensitivity responses of 78.8%, 77.8%, and 69.7% respectively at 1.3 THz. The study also discusses the optimization of key parameters to achieve high performance, offering significant insights into THz spectrum chemical sensing applications [22]. The document presents a study on designing a PCF optimized for detecting Hydrogen Cyanide (HCN) gas, focusing on achieving high sensitivity and low confinement loss. The proposed PCF features circular air hole layers around the core, utilizing Finite Element Method (FEM) simulations to predict its performance. Results indicate a high relative sensitivity (65.13%) and low confinement loss (1.5×10^{-3} dB/m) at a 1.533 µm wavelength, suggesting its suitability for industrial and medical applications requiring HCN detection [5]. Rakib Hossen et al. discusses a novel PCF design for detecting alcohols like ethanol, butanol, and propanol using THz spectrum sensing. Utilizing a hexahedron core and heptagonal cladding with circular air holes, the PCF demonstrates high sensitivity and low confinement losses at 1 THz, making it suitable for various applications, including the food and beverage industry. The study highlights the potential of this PCF sensor in improving safety protocols by efficiently detecting alcohol in beverages [23].

Shuvo Sen et al. discusses the design and simulation of a Zeonex-based Decagonal Photonic Crystal Fiber (D-PCF) for chemical sensing in the THz range. It showcases the sensor's high relative sensitivity and low confinement losses for detecting ethanol, benzene, and water. Utilizing FEM simulations, the study demonstrates the D-PCF's potential for industrial and biomedical applications, particularly in gas sensing, by achieving better performance metrics compared to previous designs [10,16-26].

Ahmmed A. Rifat et al. reviews on Photonic Crystal Fiber (PCF) based plasmonic sensors, highlighting their development for enhanced sensitivity and specificity in detecting chemical and biological analytes. It delves into the fundamentals of PCF technology and Surface Plasmon Resonance (SPR), outlining the advantages of PCF-SPR sensors over conventional methods. The review discusses various designs, fabrication techniques, and the potential future directions for these sensors, emphasizing their applications in fields like medical diagnostics, environmental monitoring, and food safety. It identifies current challenges in scaling up these technologies for commercial use and suggests pathways for future research [9]. Md. Saiful et al. presents a study on PCF based sensors for detecting toxic chemicals, specifically focusing on cyanide detection in the THz frequency band. Utilizing Zeonex as the substrate, the research designs and evaluates two types of PCFs with different core structures for improved sensitivity and reduced fabrication complexity. The study highlights the potential of these sensors in industrial and medical applications for efficient and flexible detection of highly toxic substances, demonstrating the feasibility of fabrication with existing technologies [12] **(Figure 1)**.

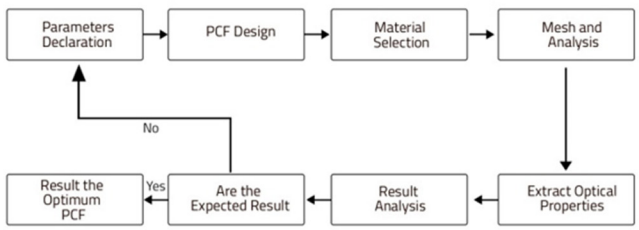

Figure 1: Block diagram representing the sequential steps of the sensor model design and analysis.

Materials and Methods

Sensor design and theoretical modelling

In this study, we propose a straightforward PCF oil-sensor model to overcome manufacturing difficulties and enhance relative sensitivity with minimal effective material loss. To find the appropriate design parameters that enable higher sensing qualities, we varied the strut size and simulation frequencies. It is simpler to

incorporate a large volume of sensing material into the core of the suggested oil-sensor since the core region is made up of hexagonal hole. Moreover, the ideal strut size and circular and hexagonal air holes across the sensor significantly reduce the effect of fiber material on the sensor's wave-guiding capabilities [1] **(Figure 2)**.

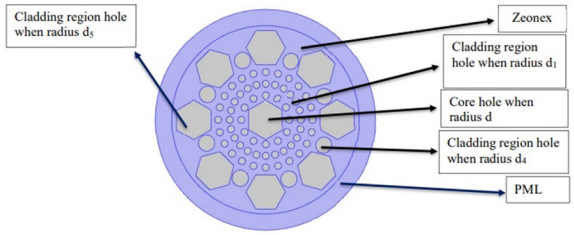

Figure 2: Designed view of proposed hollow core-based PDC edible oil detection sensor in two dimensions.

The proposed hollow-core PCF features a single hexagonal-shaped air hole in the core of its structure, as shown in **Figure 2**. The radius of the core is d=170 um. The cladding is the external ring of the fiber. This region is constituted with few layers of dielectric medium. Here perfectly three circular types air holes and one hexagonal shaped air holes are playacting the role of the dielectric medium. Total 4 layers air holes are utilized to accomplish the shape. The first layer of the cladding is formed with 12 and 12 air holes consist of 30°, 60°, 180°, 160°, 190°, 230°, 270°, 310°, 350°. Second layer is formed with 24 air holes, third layer is formed with 24 circular air holes and fourth layer is formed 8 circular air holes and 8 hexagonal air holes. The radius of first to third layer air holes are d_1= d_2= d_3=30 um and fourth layer circular air holes radius are d_4=70 um and hexagonal air holes radius are d_5=170 um. The distance of first layer from core is 210 um. Again, the distance form first layer to second layer, second layer to third layer, third layer to fourth layer is 100 um. In order to prevent back-reflection, a circle Perfectly Matched Layer (PML) is placed at the fiber's external surface. This layer's function is to absorb light that leaks from the cladding's exterior surface. Zeonex was used as the ambient substance for the alleged oil detector due to its lowest loss and the most stable index of refraction (n=1.53) between 0.1 and 3 THz. Zeonex is selected as the sensor's component because it has the maximum refractive index and transparency in the THz frequency range **(Figures 3-5)**.

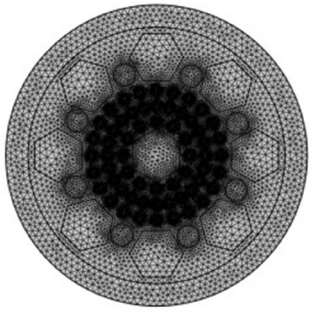

Figure 3: Meshing output with boundary condition of the suggested sensor.

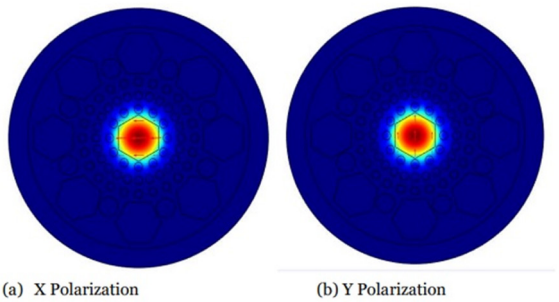

Figure 4: Light confinement in the PCF-based oil detection of the proposed sensor's core.

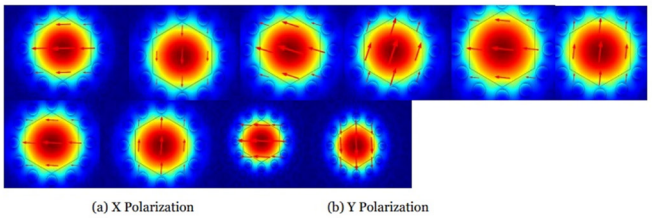

Figure 5: Light mode distribution of PCF-based oil detection of proposed sensor. The light modes variation of the PCF sensor at x-pol and y-pol, respectively, is shown infigs 5(a) and 5(b), when the proposed sensor is filled with sunflower, mustard, olive and palm oil, in that order. All the figures showed that the light is highly restricted within the core, which is required for high sensitivity.

Mathematical analysis

A simulation tool that is based on the Full Vector Finite Element Technique (FV-FEM) is used to both develop and analyze the PCF sensor that was previously demonstrated. The PCF sensor is evaluated against with a range of frequencies (i.e., 1.0 THz ≤ f ≤ 3.0 THz) once the sensor structure is complete, the materials have been chosen, and the mesh analysis has been performed.

The parametric investigation of relative sensitivity, core power, effective area, nonlinearity, and Effective Material Loss (EML) is discussed in this piece. The Beer-Lambert law explains that the strength of radiation-matter interaction determines the sensitivity of the oil adulteration sensor. This working principle is used for the suggested sensor, where the measurements rely on the changes in the absorption coefficient at a specific frequency, as shown in equation (1).

$$I(f) = L_0(f)e^{-r\alpha_m l_c} \quad \text{..... (1)}$$

Where I(f) denotes the intensity of the radiation when the THz waveguide is filled with the SUT, L_0 (f) is the intensity without the presence of SUT, r is the relative sensitivity of the sensor, α_m is the absorption coefficient andl_c is the length of the waveguide. Relative sensitivity is the most important characteristic since it represents the sensor's ability to detect changes in the SUT (Sample Under Test).

A PCF fiber's Effective Area (EA) is an essential optical feature. We previously learned that the PCF configuration with a wider

EA exhibits greater Relative Sensitivity (RS). Thus, the EA was calculated using the following equation [27]:

$$A_{eff} = \frac{[\int\int I(rd)rddrd]^2}{[\int I^2(rd)drd]^2}, (m^2) \quad \ldots\ldots\ldots\ldots\ldots (2)$$

Where, A_{eff} is the effective area, I (r) is the cross-sectional electric field intensity, and $I(rd)=|E_t|^2$.

We knew that the PCF structure is where the whole power is transmitted. Now, we use the subsequent equation to get the total Power Fraction (PF) [28].

$$\eta = \frac{\int_i S_z dA}{\int_{all} S_z dA} \quad \ldots\ldots\ldots\ldots (3)$$

In this instance, η displays the total power fraction, the core or cladding area is represented by the nominator integration. The total cross-sectional area is also determined by adding the pointing vector to the denominator S_z .

Confinement loss is another key factor of the PCF structure's optical characteristics. Moreover, the PCF based on less Confinement Loss (CL) has a better RS to detect the substances quickly. Here, the CL is calculated using the equation shown in (3):

$$L_c = 8.686 \times K_0 \, Im\,[n_{eff}]\ (dB/m) \quad \ldots\ldots\ldots\ldots (4)$$

Here, $K_0 = \left(\frac{f}{c}\right)$, the photon's speed is c, and the frequency is f. Furthermore, the effective refractive index, represented by the imaginary component I_m (n_{eff}).

To detect the substances in a PCF structure, the relative sensitivity is the most important optical property. Therefore, we use the following mathematical expression to compute the RS [1]:

$$R = \frac{n_r}{n_{eff}} \times E \quad \ldots\ldots\ldots (5)$$

Where, n_r and n_{eff} respectively represent the (RI) and Effective Refractive Index (ERI). Moreover, the total interaction between matter and light is estimated as [1],

$$E = \frac{\int_{sample} Re(E_x H_y - E_x H_y)dxdy}{\int_{total} Re(E_x H_y - E_x H_y)\,dxdy} \times 100\ \% \quad \ldots\ldots (6)$$

E_x and E_y represent the electric fields of the x and y elements, whereas H_x and H_y represent the magnetic fields of the x and y modes.

Results and Discussion

The suggested wave guide electric field propagation is evaluated utilizing FEM along with the core through the Sample Under Test (SUT). **Table 1** shows the refractive index data for several oil sample types at room temperature. The basic components of this type of sensing device include a terahertz light source, an optical detector, a spectral analyzer, and a display unit. A laser light source with a limited bandwidth and an isotonic mixture of the testing data are required for optimal accuracy. Prior to turning on the light source, the data will be inserted into the core using any common technique. When the light beam has passed through into the wave guide and been detected by the photo detector, the analyzer will measure its power and determine its effective refractive index. Consequently, the required mathematical equations will be input into a computer, which will calculate the relative sensitivity of a suggested sensor and other guiding factors.

Table 1: Refractive indices of different oil samples are under test at room temperature.

Oil type	Refractive index
Sunflower oil	1.4735
Mustard oil	1.476
Coconut oil	1.463
Olive oil	1.466
Palm oil	1.454

Measurement of the efficiency of our suggested oil sensor in relation to both frequency and design layout. The hexagonal core's diameter, which is set 170 um, is primarily considered to be a measure of the relative sensitivity of the sensor. The research is conducted at a 2, 2.1, 2.2 THz frequency response. According to **Figure 4**, the relative sensitivities of the suggested sensors—is 85.59%, 84.65%, 82.68%, respectively at f=2.2 THz, for several types of sunflower oil, mustard oil, olive oil and 82.63% at f=2.1 for coconut oil and 79.65% at f=2 THz for palm oil.

Figure 6 displays the suggested sensor's relative sensitivity at 170 µm core diameter for different working modes. Around 1 to 3 THz, the relative sensitivity increases fast, then decreases until it becomes almost consistent for all kinds of oils around 2.2 THz. When several lights propagate through the large indexed test because of the larger frequency electromagnetic wave's ability to cross greater indexed zones, the sensitivity rises. Here to maximum of our understanding, neither any findings have been published in the field that are greater than the relative sensitivity from over 85.59%, for all trials of the proposed sensor.

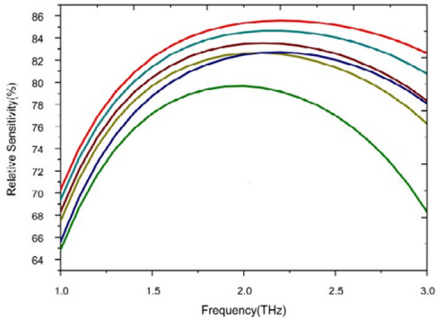

Figure 6: The relative sensitivity variation with frequency for different oil samples over the frequency ranging from 1.0 to 3.0 THz. **Note:** (—) Sunflower oil X-Pol; (—) Sunflower oil Y-Pol; (—) Mustard oil X-Pol; (—) Mustard oil Y-Pol; (—) Coconut oil X-Pol; (—) Coconut oil Y-Pol; (—) olive oil X-Pol; (—) olive oil Y-Pol; (—) Palm oil X-Pol; (—) Palm oil Y-Pol.

The EML design of the suggested sensor based on different core diameters and operating frequencies is depicted in **Figure 7**, accordingly. The above graphs demonstrate that EML at 2.2 THz decreases as core diameter increases because less resistivity can propagate across an expanding core. Consequently, the transfer of energy is decreased, and a small amount of light is retained by the solid material. The EML ranges from around 0.02561

cm^{-1}, 0.035427cm^{-1} for various oil samples at the ideal core diameter, which is a narrow region. Nevertheless, oil with a more refractive index has a less EML because it permits lighter to travel through it under constant operating conditions than oil with a smaller refractive index. The sensor exhibits comparable sorts of characteristics at various operating frequencies, as illustrated in **Figure 7**. A smaller amount of light is captured by the solid substance between the core and cladding at greater frequencies because less light passes through the low indexed cladding area. This explains why higher frequencies have a smaller loss. The EML of the provided sensor is less than 0.02561 cm^{-1} at 2.2 THz range and 170 um core diameters.

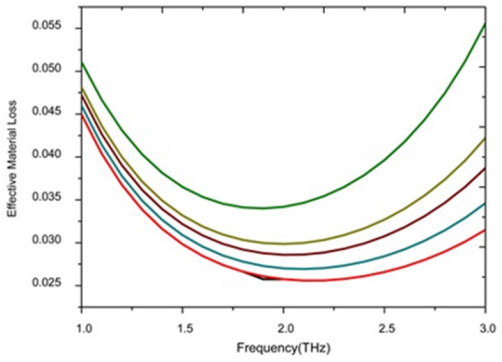

Figure 7: The EML variation with frequency fora different oil samples over the frequency ranging from 1.0 to 3.0 THz. **Note:** (▬) Sunflower oil X-Pol; (▬) Sunflower oil Y-Pol; (▬) Mustard oil X-Pol; (▬) Mustard oil Y-Pol; (▬) Coconut oil X-Pol; (▬) Coconut oil Y-Pol; (▬) olive oil X-Pol; (▬) olive oil Y-Pol; (▬) Palm oil X-Pol; (▬) Palm oil Y-Pol.

For different core diameters and working frequencies, **Figure 8** shows the CL profile of the suggested oil sensor. In both cases, the amount of loss decreases when the x-axis parameter is increased because wider and higher-frequency cores enable larger amounts of light to reach the core. The suggested sensors CL for sunflower oil, muster oil, coconut oil, and olive oil is 1.55 × 10^{-8} dB/m, 1.63 × 10^{-8} dB/m, 1.31 × 10^{-8} dB/m, 1.99 × 10^{-8} dB/m, 4.0345 × 10^{-8} dB/m, respectively, at the optimal core diameter (170 um) and operating frequency (2.2 THz).

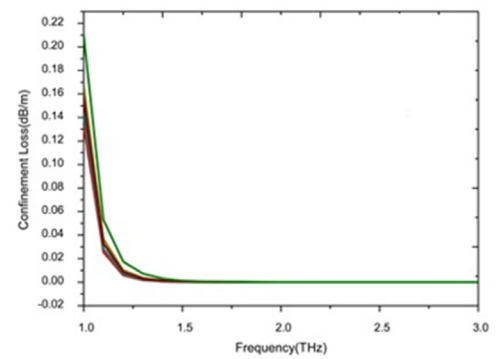

Figure 8: The CL variation with frequency for different oil samples over the frequency ranging from 1.0 to 3.0 THz. **Note:** (▬) Sunflower oil X-Pol; (▬) Sunflower oil Y-Pol; (▬) Mustard oil X-Pol; (▬) Mustard oil Y-Pol; (▬) Coconut oil X-Pol; (▬) Coconut oil Y-Pol; (▬) olive oil X-Pol; (▬) olive oil Y-Pol; (▬) Palm oil X-Pol; (▬) Palm oil Y-Pol.

The EML and CL are the two main losses in PCF-based sensors, as was before mentioned. The entire loss caused by the suggested sensor is shown in **Figure 9**. The overall losses provided by the sensor under ideal circumstances for various types of oil samples are 1.55 × 10^{-8} dB/m, 1.63 × 10^{-8} dB/m, 1.31 × 10^{-8} dB/m, 1.99 × 10^{-8} dB/m, 4.0345 × 10^{-8} dB/m respectively. This is better than the results of earlier studies [6-10,28].

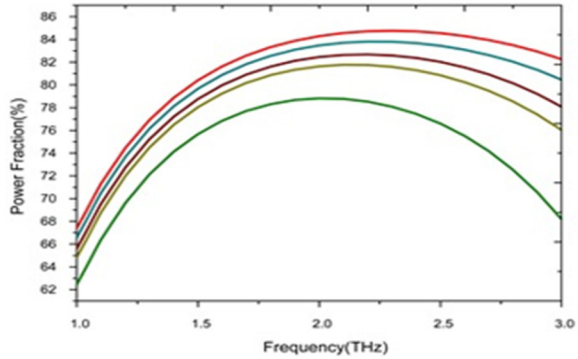

Figure 9: The power fraction variation with frequency for different out samples over the frequency ranging from 1.0 to 3.0 THz. **Note:** (▬) Sunflower oil X-Pol; (▬) Sunflower oil Y-Pol; (▬) Mustard oil X-Pol; (▬) Mustard oil Y-Pol; (▬) Coconut oil X-Pol; (▬) Coconut oil Y-Pol; (▬) olive oil X-Pol; (▬) olive oil Y-Pol; (▬) Palm oil X-Pol; (▬) Palm oil Y-Pol.

A smaller effective area results from the light confinement becoming more concentrated at increasing operating frequency, f. When the frequency is increased from 0.9 THz to 2 THz, **Figure 9** shows the effective area of the photonic crystal fiber for the ideal core diameter. According to the graph, the operation frequency and effective area are inversely connected. Within a constrained area of the fiber sensor, a high-frequency electromagnetic signal is produced. The effective area of the suggested sensor is around 6.83 × 10^{-8} μm^2 for all oil samples under optimum working circumstances, which is highly useful.

To compare the sensing and controlling qualities of the proposed sensor with the previously suggested PCF-based sensors, a comparison table **(Table 2)** is calculated. The following table shows that, in terms of relative sensitivity, the suggested sensor outperforms the presented chemical/liquid sensor by a significant amount. Subsequently a feasible way of manufacturing the suggested sensor is studied **(Figures 10-12)**.

Additionally, a variety of asymmetrically constructed PCFs have been created in the laboratory utilizing a variety of building techniques. It is evident from a detailed examination of those fibers that the manufactured PCFs are very comparable to our modeled PCF. Therefore, it is evident that a hybrid PCF may be made using the stack and sketch approach with respectable precision [29,30]. When comparing the structure of our suggested PCF to that of the previously reported PCFs, it becomes clear that the suggested fiber may be generated in the laboratory with minimal difficulty. The suggested PCF's ideal fiber dimensions are close to 1.66 mm, indicating that the proposed sensor may be simply constructed in the laboratory. For this purpose, we advise employing the stack-and-draw technique to create these

specialty fibers, since it allows for the accurate production of all PCF kinds in the laboratory environment.

From the table, our suggested oil sensor may result in a lower EML. Additionally, this sensor now has significantly better sensitivity, demonstrating the suitability of the sensor as it is currently being offered.

Table 2: Comparison of sensing and guiding characteristics of PCF-based sensors.

Ref	Finalized frequency(f)/ wavelength(λ)	Sensing sample	Relative sensitivity	Effective area	Effective material loss	Confinement Loss (dB/m)
22	f=1.3 THz	Ethanol	78.80%	–	0.0501 cm^{-1}	
		Benzene	77.80%			
		water	69.70%			2.19×10^{-10}
28	f=2.0 THz	camel	81.16%	–	0.033 cm^{-1}	8.675×10^{-18} cm^{-1}
		cow milk	81.32%		0.032824 cm^{-1}	0.435×10^{-18} cm^{-1}
30	f=1.0 THz	Ethanol	68.87%	–	–	7.79×10^{-12} cm^{-1}
31	λ =1.33 µm	Ethanol	53.22%	93,800 um^2	0.03301 cm^{-1}	–
		Water	48.19%			
		Benzene	55.56%			
16	λ=0.6 um-1.3 um	Human mucosa	47.31%	–	–	–
		Glucose	47.59%			
11	f=1.0 THz	Ethanol	78.56%	–	–	6.02×10^{-8} dB/m
		Benzene	79.76%			5.80×10^{-8} dB/m
		water	77.51%			5.74×10^{-8} dB/m
23	λ=1.533 µm	Hydrogen cyanide gas	65.13%	–	–	1.5×10^{-3} dB/m
This work 2024	f=2.2 THz	sunflower oil	85.59%	7.22×10^{-8} m^2	0.02561 cm^{-1}	1.55×10^{-8} dB/m
		mustard oil	84.65%	7.09×10^{-8} m^2	0.027054 cm^{-1}	1.63×10^{-8} dB/m
		coconut oil	82.63%	6.83×10^{-8} m^2	0.030322 cm^{-1}	1.31×10^{-8} dB/m
		olive oil	82.68%	7.09×10^{-8} m^2	0.028854 cm^{-1}	1.99×10^{-8} dB/m
		palm oil	79.16%	6.5231×10^{-8} m^2	0.035427 cm^{-1}	4.0345×10^{-8} dB/m

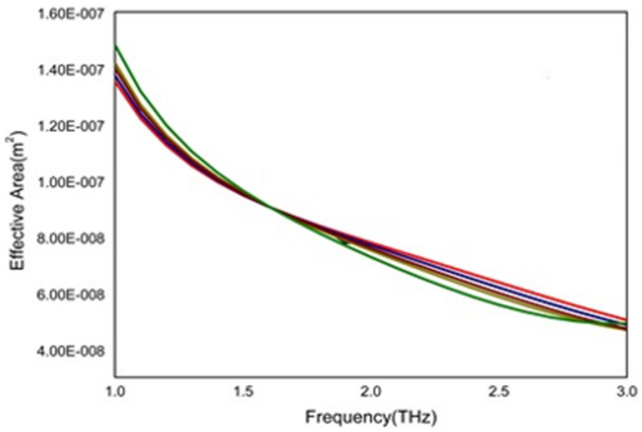

Figure 10: The effective area variation with frequency for different oil samples over the frequency ranging from 1.0 to 3.0 THz. **Note:** (▬) Sunflower oil X-Pol; (▬) Sunflower oil Y-Pol; (▬) Mustard oil X-Pol; (▬) Mustard oil Y-Pol; (▬) Coconut oil X-Pol; (▬) Coconut oil Y-Pol; (▬) olive oil X-Pol; (▬) olive oil Y-Pol; (▬) Palm oil X-Pol; (▬) Palm oil Y-Pol.

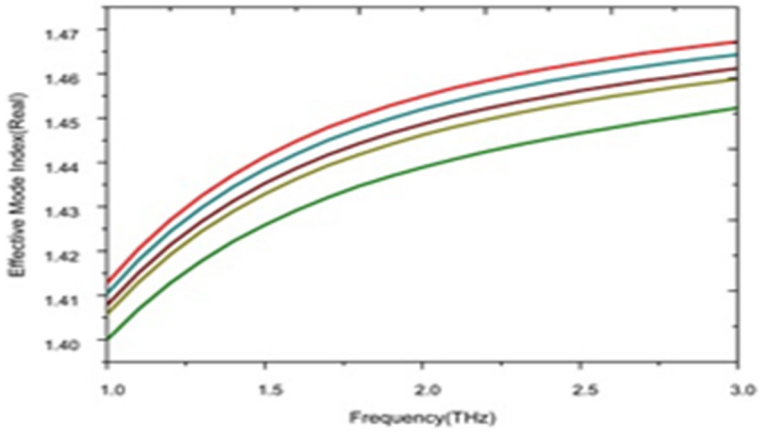

Figure 11: Change of effective refractive index (real) with increasing frequency from 1.0 to 3.0 TH z for different oil samples. **Note:** (▬) Sunflower oil X-Pol; (▬) Sunflower oil Y-Pol; (▬) Mustard oil X-Pol; (▬) Mustard oil Y-Pol; (▬) Coconut oil X-Pol; (▬) Coconut oil Y-Pol; (▬) olive oil X-Pol; (▬) olive oil Y-Pol; (▬) Palm oil X-Pol; (▬) Palm oil Y-Pol.

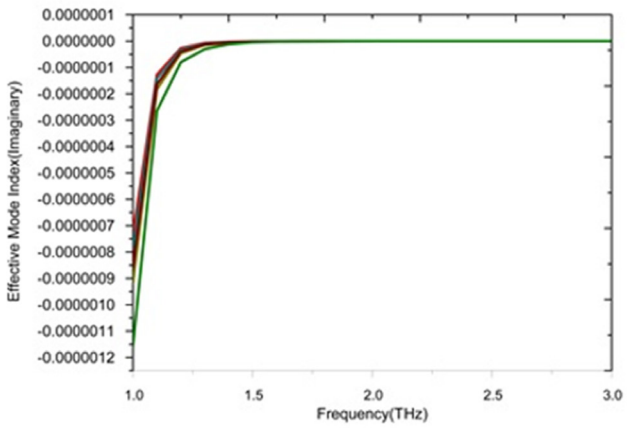

Figure 12: Change of effective refractive index (imaginary) with increasing frequency from 1.0 to 3.0 THZ for different oil samples. **Note:** (▬) Sunflower oil X-Pol; (▬) Sunflower oil Y-Pol; (▬) Mustard oil X-Pol; (▬) Mustard oil Y-Pol; (▬) Coconut oil X-Pol; (▬) Coconut oil Y-Pol; (▬) olive oil X-Pol; (▬) olive oil Y-Pol; (▬) Palm oil X-Pol; (▬) Palm oil Y-Pol.

Conclusion

Edible oil that is pure and nourishing contributes to a safe and healthy lifestyle. On the other hand, some dishonest traders profit more by selling inferior oil, even at the risk of their customers' health. Therefore, before edible oil is consumed by humans, it is imperative to evaluate its quality. Therefore, a completely new structural PCF is suggested in this research to detect various food oils utilizing THz signals. Our proposed sensor offers a promising opportunity to advance oil sensing capabilities using photonic crystal fiber technology. Based on the numerical computations, the proposed sensor exhibits a relative sensitivity of 85.591%, 84.648%, 82.625%, 82.683%, and 79.161% for sunflower, mustard, coconut, olive and palm oil respectively at 2.2 THz. Furthermore, under ideal geometric conditions, the fiber achieves minimal confinement loss and a low effective material loss of 0.02561 cm^{-1}. Due to its high sensitivity and straightforward form, we strongly believe that the proposed sensor will be an effective device in the field of oil detection technologies.

References

1. Islam MN, Al-tabatabaie KF, Habib MA, Iqbal SS, Qureshi KK, et al. (2022) Design of a hollow-core photonic crystal fiber based edible oil sensor. Crystals 12:1362.
2. Johny J, Prabhu R, Fung WK (2016) Investigation of structural parameter dependence of confinement losses in PCF–FBG sensor for oil and gas sensing applications. Opt Quantum Electron 48:1-9.
3. Ferdous AHMI, Anower MS, Habib MA (2021) A hybrid structured PCF for fuel adulteration detection in terahertz regime. Sens Bio-Sensing Res 33:100438.
4. Ferdous AI, Anower MS, Musha A, Habib MA, Shobug MA (2022) A heptagonal PCF-based oil sensor to detect fuel adulteration using terahertz spectrum. Sens Bio-Sensing Res 36:100485.
5. Liu S, Liu J, Li Y, Zhang J (2021) THz sensor based on dual-core PCF with defect core in detecting adulteration of olive oil. Opt. Quantum Electron 53:1-10.
6. Ferdous AHMI, Anower MS, Habib MA (2021) A hybrid structured PCF for fuel adulteration detection in terahertz regime. Sens Bio-Sensing Res 33:100438.
7. Paul AK (2020) Design and analysis of photonic crystal fiber plasmonic refractive Index sensor for condition monitoring of transformer oil. OSA Continuum 3:2253-2263.
8. Wang Y, Ma G, Zheng D, Liao W, Jiang J, et al (2020) Detection of dissolved acetylene in power transformer oil based on photonic crystal fiber. IEEE Sens J 20:10981-10988.
9. Islam MS, Ferdous AI, Tamilselvi M, Swarna M, Anitha G, et al. (2023) Highly sensitive hybrid structured based dodecagonal core with double layer hexagonal cladding photonic crystal fiber for food oil health sensing. J Opt 1-15.
10. Hossen R, Md Selim Hossain, Sabbir Ahmed, Mohammad Sayduzzaman, Marjia Sultana, et al. (2023) Design and performance analysis of alcohols sensing using photonic crystal fiber in terahertz spectrum. Open Phys J 17:100192.
11. S Sen, Md Abdullah-Al-Shafi, A S Sikder, Md S Hossain, MM Azad (2021) Zeonex based Decagonal Photonic Crystal Fiber (D-PCF) in the Terahertz (THz) band for chemical sensing applications. Sens Bio-Sensing Res 31:100393.
12. Almawgani Abdulkarem HM, Alhamss Dana N, Taya Sofyan A, Hindi Ayman Taher, Upadhyay Anurag, et al. (2023) Identification of four detrimental chemicals using square-core photonic crystal fiber in the regime of THz. J Appl Phys 133:24.
13. Rifat AA, Rajib Ahmed, Ali K Yetisen, Haider Butt, Aydin Sabouri et al. (2017) Photonic crystal fiber based plasmonic sensors. Sens Actuators B: Chem 243:311–325.
14. Md S Islam, J Sultana, A Dinovitser, K Ahmed, BW H Ng, et al. (2018) Sensing of toxic chemicals using polarized photonic crystal fiber in the terahertz regime. Opt. Commun 426:341–347.
15. Md S Hossain, R Hossen, S T Alvi, Md S Hossain, M. Al-Amin (2023) Design and numerical analysis of a novel photonic crystal fiber based chemicals sensor in the THz regime. Open Phys J 17:100168.
16. JBM Leon, S Abedin, Md A Kabir (2021) A photonic crystal fiber for liquid sensing application with high sensitivity, birefringence and low confinement loss. Sensors International 2:100061.
17. Wakf AME, Hassan HA, Gharib NS (2013) Osteoprotective effect of soybean and sesame oils in ovariectomized rats *via* estrogen like mechanism. Cytotechnology 66:335–343.
18. Fusaro M, Mereu MC, Aghi A, Lervasi G, Gallieni M (2017) Vitamin K and bone health. Clin Cases Miner Bone Metab 14:200–206.
19. Berger ME, Smesny S, Kim SW, Davey CG, Rice S, et al. (2017) Omega-6 to omega-3 polyunsaturated fatty acid ratio and subsequent mood disorders in young people with at-risk mental states: A 7 year longitudinal study. Transl Psychiatry 7:1220.
20. Md B Hossain, J Kříž, V Dhasarathan, Md E Rahaman (2023) Photonic Crystal Fiber (PhCF) for petrochemical sensing. Front Phys 10.
21. I S Amiri, K Ahmed, V Dhasarathan, F Ahmed, S Roy, et al. (2018) Quasi-photonic crystal fiber based spectroscopic chemical sensor in the terahertz spectrum: Design and analysis. IEEE Sens J 18:9948–9954.
22. A E Fard, S Makouei, M Danishvar, S Daneshvar (2024) The design of a photonic crystal fiber for hydrogen cyanide gas detection. Photonics 11:178.

23. Rahman MM, Mou FA, Bhuiyan MIH, Islam MR (2020) Photonic crystal fiber based terahertz sensor for cholesterol detection in human blood and liquid foodstuffs. Sens Biosensing Res 29:100356.

24. Geng Y, Wang L, Xu Y, Kumar AG, Tan X et al. (2018) Wavelength multiplexing of four-wave mixing based fiber temperature sensor with oil-filled photonic crystal fiber. Opt. Express 26:27907-27916.

25. Bulbul AAM, Rashed ANZ, El-Hageen HM, Alatwi AM (2021) Design and numerical analysis of an extremely sensitive PCF-based sensor for detecting kerosene adulteration in petrol and diesel Alex Eng J 60(6):5419-5430.

26. Ferdous AI, Sarker P, Hasan MG, Islam MA, Musha A, et al. (2023) Design of a terahertz regime-based surface plasmon hybrid photonic crystal fiber edible oil biosensor Plasmonics 18:1923-1932.

27. M Islam, MR Islam, S Sir az, M Rahman, MS Anzum, et al. (2021) Wheel structured Zeonex-based photonic crystal fiber sensor in THz regime for sensing milk. Appl Phys A 127(5):1–3.

28. Jakeya Sultana, Md Saiful Islam, Kawsar Ahmed, Alex Dinovitser, brian W-H Ng, et al. (2018) Terahertz detection of alcohol using a photonic crystal fiber sensor Appl Opt 57(10):2426-2433.

29. Md Shadidul Islam, Bikash Kumar Paul, Kawsar Ahmed, Sayed Asaduzzaman, Md Ibadul Islam, et al. (2017) Liquid-infiltrated photonic crystal fiber for sensing purpose: Design and analysis. Alex Eng J 57(3):1459-1466.

30. Reza MS, Habib MA (2020) Extremely sensitive chemical sensor for terahertz regime based on hollow-core photonic crystal fiber Ukranian J Phys Opt 218–14.